

Colloidal model system for island formation

D Deb and H H von Grünberg

Institut für Chemie, Karl-Franzens Universität Graz, A-8010 Graz, Austria

Received 13 March 2009, in final form 15 April 2009

Published 12 May 2009

Online at stacks.iop.org/JPhysCM/21/245102

Abstract

We present model calculations to explore the possibility of colloidal island formation over strained surfaces. Colloids, aggregating due to attractive depletion interactions, are deposited onto a colloidal surface whose lattice constant and geometry can be varied by optical forces. This allows precise control of the strain between the substrate and the colloidal adsorbate. Three different strain fields are considered: fields with either an unidirectional or a hexagonal variation of strain, and fields with a combination of both variations. We find that the unidirectional field induces the formation of infinitely extended ridges, while hexagonal strain fields lead to regular pyramidal island structures which can be distorted in a controlled way by adding the unidirectional strain component. We furthermore study the dependence of island size on strain strength for the hexagonal strain pattern and find that the area occupied by an island is a constant fraction of the strain field's repeat unit.

(Some figures in this article are in colour only in the electronic version)

1. Introduction

Over the last ten years two-dimensional (2D) colloidal crystals have become a popular system for various studies on solid state phenomena. Recent papers on 2D colloidal crystals include the experimental verification of the classical Kosterlitz–Thouless–Halperin–Nelson–Young theory of 2D melting [1–5], measurements of both over-damped phonon dynamics [6] and dispersion curves [7], investigations on the melting properties of anisotropic crystals [8, 9], but also papers on such varying topics as point-defect dynamics [10], dislocation interaction [11] or structural transitions between different lattices [12].

Having explored the properties of 2D colloidal crystals as such, related research activities now seem to be developing in two different directions. Quenching 2D colloidal fluids allows the production of glassy colloidal monolayers—an ideal playground to learn more about the glass transition [13] or the ripening of crystallites [14]. Another perspective of further research has opened following the invention of artificial substrate potentials which 2D colloidal crystals can be exposed to. These substrate potentials can be created in several different ways (see the review [15]), most importantly, by means of optical tweezers [16]. In the latter case, a number of different laser beams are brought to interference [17] such that spatially extended standing light-fields are formed that act as an external periodic potential for the colloidal monolayer

system. Its periodicity can be conveniently controlled by the geometry of the incident light pattern [15]. Equally convenient to control is the colloid density which in modern colloid experiments is changed by system-confining optical line traps [18]. In addition, the colloidal monolayer is subjected to a vertical light pressure, which is counterbalanced by the electrostatic repulsion between the like-charged glass and colloid surfaces [19, 20], such that the system is confined in a 2D plane with out-of-plane fluctuations of less than 100 nm [15].

It is obvious that 2D colloids exposed to such light-induced substrate potentials can be considered as model systems for atomic monolayers on real solid surfaces. However, the additional experimental freedom to vary *in situ* both substrate lattice geometry and lattice constant makes the composite system of substrate plus 2D colloidal crystal a unique system and clearly distinguishes it from the classical system of atoms on surfaces.

2. Background: colloidal systems interacting with light-induced substrates

To sketch the state-of-the-art of the field we briefly mention the most important studies on 2D colloid crystals interacting with light-induced substrates. This provides useful background information, but also supports our claim that the present study on colloidal island formation can be considered the next logical

step on our way from colloidal monolayers towards self-assembled 3D colloidal structures.

A *one-dimensional substrate* potential results from the gradient forces of two interfering laser beams. A number of interesting ordering phenomena have been studied for 2D colloids interacting with such 1D substrates, such as, for instance, phenomena like light-induced freezing [17], melting [21, 22] and re-entrant melting [23–25].

The interference of three laser beams is sufficient to produce *two-dimensional substrates* [16]. Brunner *et al* [26] have studied 2D colloidal systems in the presence of such 2D potentials, in a situation where two or more colloids assemble at one lattice site of the substrate potential. The resulting new structural entities are referred to as ‘colloidal molecules’ [27]. Phase behavior and orientational ordering of these colloidal molecular crystals on triangular light lattices, as measured by Brunner *et al* [26], have later been interpreted in terms of spin models [28–31]. Other colloid experiments on 2D substrates have focused on (i) the transition from an incommensurate to a commensurate colloidal solid [32], (ii) strain-induced domain formation [33] and (iii) the controlled manipulation of the crystal’s phonon band structure through the variable substrate properties [34, 35]. Recent simulation studies suggest a number of further colloid experiments in this direction, exploring the behavior of 2D colloidal crystals on *disordered substrate* potentials, i.e. in particular, the dynamics [36], the melting properties [37], the behavior in narrow channels [38] and the phase behavior [39] of these crystals.

The most recent studies use five interfering laser beams to create *quasi-crystalline deconal substrate* potentials which, when interacting with the colloidal monolayer, give rise to a rich and fascinating phase behavior [40–42].

3. Colloidal island formation

In a continuation of these activities we here suggest another colloid experiment in which the important step is made from a 2D monolayer towards colloidal growth into the third spatial dimension in the form of islands. We present model calculations with which we study the principles of island formation in colloidal adsorbates on light-induced periodic substrates.

Thin layers adsorbed on crystalline surfaces are usually strained owing to their lattice mismatch with respect to the substrate. Island formation is one possible way for an adsorbate to release this strain. Beyond a certain threshold coverage, the epitaxial system can maintain a lower energy by transferring particles from the island edge to the upper layer because the transition leads to a decrease in the contact area between the substrate and the adsorbate [43–45]. Thus, particle transitions to the upper layers lead to a relaxation in the local strain field. The trade-off between the cost of the additional surface energy and the gain of energy due to elastic relaxation is the driving force behind the island formation, resulting in island shapes that can range from flat pyramids to sharp domes [46, 47].

The main component of a colloid experiment fit for a study of island formation is the substrate, which we here suggest to

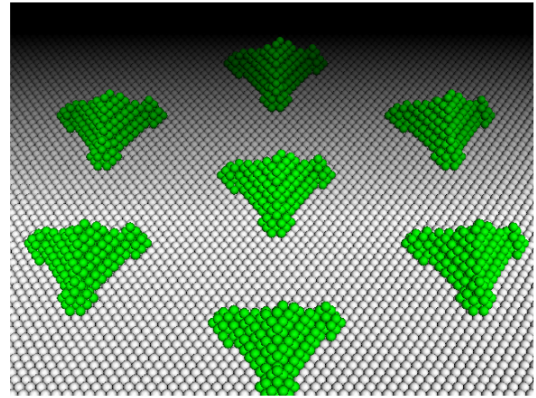


Figure 1. Landscape of colloidal islands over a substrate surface, as obtained from the model calculation presented in this work. The white colloidal spheres fixed at the minima of a light-induced potential form a substrate with variable lattice constant and island-forming green spheres are the colloids deposited over the substrate.

prepare by means of a system of colloidal spheres fixed to their positions through the deep minima of a periodic light-induced substrate potential. Variation of the periodicity of the light-field will allow control of the lattice constant within the colloidal substrate monolayer. An additional layer of the same colloids deposited onto this substrate must then be subject to a substantial strain with respect to the substrate which, under certain circumstances, will lead to the formation of islands (see below). For illustrative purposes, a landscape of colloidal islands grown over such a substrate is shown in figure 1. The important point here is that, while in atomic systems the substrate periodicity is fixed by the microscopic nature of the surface, the strain in this colloid experiment can be precisely controlled by variation of the lattice constant of the light-induced periodic potential. The control of the strain then represents a new experimental parameter to influence and manipulate colloidal island growth. Due to this additional experimental degree of freedom such a colloid experiment could help provide more insights into fundamental aspects of island formation which are difficult, if not impossible, to obtain in atomic systems, such as, for instance, the dependence of both island growth and shape evolution on (possibly rather complex) strain patterns. Also, the colloidal self-assembly process leading to the islands might be relevant for technical purposes, if one thinks, for example, of manufacturing 3D colloidal structures in large copy numbers and with a well-defined shape.

And, indeed, it is the manufacturing aspect that explains the rather widespread interest in the physics of island formation, as strained film epitaxy has become one of the most important techniques in manufacturing nanoscale materials such as semiconductor quantum dots or carbon nanotubes, with all their extraordinary functional properties (reviewed in [48]). The formation of islands—for example, islands such as quantum dots—on surfaces of epitaxially strained films result from an instability of the film. This instability has been theoretically described primarily by approaches applying continuum mechanics to study the initial film

instability [49, 50], the evolution of island shapes [51] or the additional role of a wetting interaction [52], or, alternatively, by approaches which are based on a combination of discrete microscopic and continuum elasticity descriptions [53]. Quite instructive recent examples of simulations of quantum dot island growth over a strained (and pre-patterned [45]) surface can be found in [44] or in [46] where the question is addressed of how island growth switches between pyramid and dome-like shapes as found in [47].

4. Model

4.1. The depletion potential

The second component of a colloid experiment on island formation is an attractive pair potential between the colloids. The attractiveness of the potential is essential for the aggregation process which the island formation mechanism is based on. There are several ways how one could imagine to realize such an attractive pair potential, for example, by changing the screening length in a charge-stabilized colloidal suspension such that the long-range van der Waals attraction can become effective. Another option—which we will further consider here—is to exploit the depletion interaction [54], an attractive interaction potential whose range and strength is conveniently tuned through the concentration and size of non-adsorbing polymers added to the colloidal dispersion. The depletion interaction and its effect on the topology of the phase diagram of a colloid–polymer mixture has been studied in great detail, see, for example, [55–57].

We here consider charged colloidal spheres immersed together with a non-adsorbing polymer in a common solvent. The direct pair interaction between the charged colloidal spheres with a hard-core diameter σ_c is given by

$$\beta U_{cc}(R_{ij}) = \begin{cases} \infty & \text{for } R_{ij} < \sigma_c \\ \beta \epsilon \left(\frac{\exp(-\kappa \sigma_c (R_{ij}/\sigma_c - 1))}{R_{ij}/\sigma_c} \right) & \\ \text{otherwise} & \end{cases} \quad (1)$$

where $R_{ij} = |\mathbf{R}_i - \mathbf{R}_j|$ and \mathbf{R}_i are the positions of the centers of the colloids, $\beta = 1/k_b T$ is the inverse temperature, κ is the inverse Debye screening length and ϵ determines the strength of the Yukawa interaction. The additional depletion potential arises due to the anisotropic distribution of polymer coils when two charged colloidal spheres come closer. When the separation between two colloidal spheres is less than the effective diameter of the polymer coils, the depletion of polymers in the region in between the two colloids gives rise to an attractive component in the effective pair potential between the colloids. The form of this indirect contribution to the pair potential is given by [57]

$$\beta U_{dep}(R_{ij}) = \begin{cases} \frac{\pi \sigma_p^3 \rho_p^r (1+q)^3}{6 q^3} \\ \times \left[1 - \frac{3R_{ij}}{2(1+q)\sigma_c} + \frac{R_{ij}^3}{2(1+q)^3 \sigma_c^3} \right] & \\ \text{for } \sigma_c < R_{ij} < \sigma_c + \sigma_p & \\ 0 & \text{for } R_{ij} > \sigma_c + \sigma_p \end{cases} \quad (2)$$

where σ_p is the effective diameter of the polymer coil which determines the range of the potential, ρ_p^r is the polymer density in the reservoir which affects the strength of the potential and $q = \frac{\sigma_p}{\sigma_c}$ is the size ratio of the polymer coil and colloidal sphere. Thus the total pair potential $U_{tot}(R_{ij}) = U_{cc}(R_{ij}) + U_{dep}(R_{ij})$ has a well-behaved minimum at a_0 and hence colloids in 2D interacting via such a pair potential will crystallize with a hexagonal lattice constant a_0 . To find typical values for the parameters of the pair potential of equations (1) and (2), we consulted [57] in which various different example systems are discussed, and took: $\beta \epsilon = 20$, $\kappa \sigma_c = 100$, $q = 0.2$, $\pi \sigma_p^3 \rho_p^r / 6 = 1.4$ and $a_0 / \sigma_c = 1.03$.

4.2. Preparation of strained substrates

The strained substrate is realized by placing colloids into the light-field minima and by then changing the light-field periodicity such that the hexagonal lattice constant a_S of the colloidal substrate does not match with the lattice constant a_0 which a free colloidal crystal would take. To quantify the strain we define the quantity $\lambda = (a_0 - a_S)/a_0$, which is positive (negative) if the substrate is squeezed (expanded) from its equilibrium structure. The substrate is spanned by the hexagonal unit vectors $\vec{S}_x/a_0 = \vec{e}_x \alpha_1$ and $\vec{S}_y/a_0 = \vec{e}_x (\frac{\alpha_2}{2}) + \vec{e}_y (\frac{\sqrt{3}\alpha_2}{2})$, where \vec{e}_x and \vec{e}_y are the normal rectangular unit vectors. The vector $\vec{\alpha}(\lambda) = (\alpha_1, \alpha_2, \alpha_3)$ specifies the strain pattern, which in practice can be changed by tuning the three laser beams creating the substrate potential. We consider the following three different strain patterns, depicted in figure 2: (i) an unidirectional variation of strain, $\vec{\alpha}(\lambda) = (1, 1, 1 - \lambda)$, (ii) a hexagonal strain variation, $\vec{\alpha}(\lambda) = (1 - \lambda, 1 - \lambda, 1 - \lambda)$ and (iii) a combination of both unidirectional and hexagonal strain, $\vec{\alpha}(\lambda) = (1 - \lambda, 1, 1 - \lambda)$. Note that the compressed (expanded) set of lattice lines again matches the free ones after a period length of $L = 1/\lambda$ (marked in figure 2); thus the strain field itself has a periodicity.

The algorithm for modeling the growth mechanism is as follows. We use periodic boundary conditions, with a hexagonal simulation box which is compatible with the substrate strain field. The simulation box has a side length of $2L$, as indicated in figure 2. Colloids, identical to those used to realize the substrate, are deposited over the strained substrate, one at a time. The first colloid is deposited where the strain is zero, i.e. at the center of the simulation box. The next particle is placed at a position taken from a list of trial positions which comprise possible sites within the same layer of particles, but also sites belonging already to the next layer. The new island configuration is then fed into a standard energy minimization routine, to find the energy and the relaxed positions of the new adsorbate cluster. This procedure is repeated for all trial positions on the list and the particle is finally allowed to reside on the position corresponding to the lowest overall energy. Updating the list of trial positions, one can start the next cycle by adding another colloidal particle. We have checked that, in the case of no strain, the growth develops in a layer-by-layer fashion, as it should. The simulation box was chosen substantially larger than the real repeat unit of the strain field, in order to ensure that the shape of the colloidal islands is

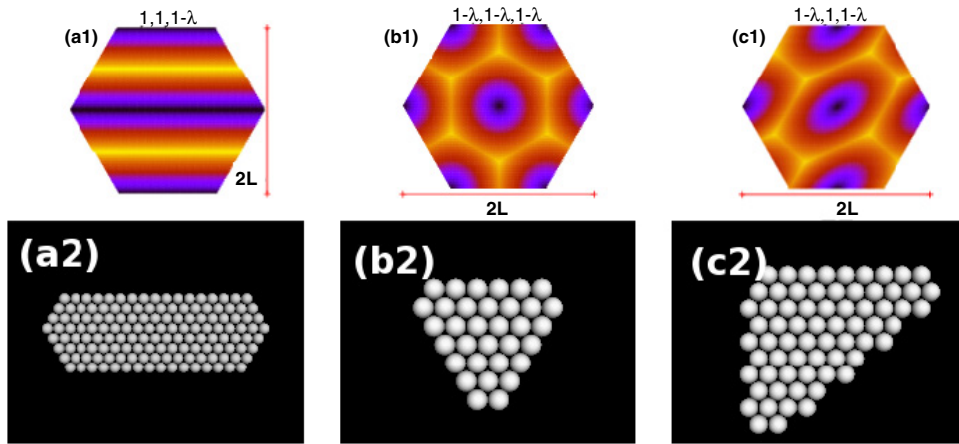


Figure 2. The three strain fields considered in this work, (a1) linear, (b1) hexagonal and (c1) distorted hexagonal, computed from the differences of the particle positions in the strained relative to an unstrained substrate. The color code goes from black (no strain) to white (maximum strain). (a2), (b2) and (c2): first layer of colloidal islands formed at the center of a hexagonal simulation box for the strain fields as given in (a1), (b1) and (c1).

determined solely by the strained substrate and not by other islands growing in the neighborhood.

In principle, the substrate colloids are subject to the same interaction potential as the adsorbing colloids; still, when performing the energy minimization they are not allowed to relax in response to the adsorbed colloids, but are assumed to be held permanently fixed at the positions given by the minima of the optical lattice. This is a reasonable assumption given the fact that the optical forces of the light-induced lattice can be tuned such that it becomes orders of magnitude larger than the intercolloidal forces [15]. The effect of an additional substrate relaxation can then be safely ignored.

5. Results and discussion

Shape of first layer. We start by discussing the geometry of the first layer of the colloidal islands resulting from the minimization procedure described above; in figure 2 these layers are confronted with their respective strain fields. For unidirectional strain, case (a2) in figure 2, the first layer closely mimics the strain field, forming infinitely extended horizontal stripes whose widths depend on the strength of the strain. For the hexagonal strain field, case (b1), a triangle with truncated vertices is obtained which can be viewed as a hexagon consisting of two types of triangles differing in their base lengths. This deformed hexagon is the result of a competition between two hexagonal structures having different lattice constants, one resulting from the free crystal and the other which is imposed by the strain field. Indeed, monitoring the layer formation process starting from the first colloid, one can observe that, in the beginning, near the zone of zero strain, the shape of the first layer remains almost perfectly hexagonal. But for a growing first layer, the effect of strain starts to prevail by restricting colloids such that the nature of the growth changes from hexagonal to triangular. Finally, the first layer formed over a substrate with a distorted hexagonal strain field in figure 2(c2) is also a capped triangle, however,

now elongated along one direction—a distortion that arises due to the additional unidirectional strain component.

Island growth paths. Figures 3–5 show the morphological evolution of the islands, for the three strain fields considered, starting from the first layers shown in figures 2(a2), (b2) and (c2). For the linear strain field in figure 3, an infinitely extended ridge forms through an fcc stacking process of layers on top of the first striped layer, until in the last layer only a single row of particles can be accommodated. Such a state of the island is shown in figure 3(b). The colloids deposited thereafter go again to the bottom layer and fill another layer on one of the facets of the already existing ridge, figures 3(c) and (d), a process which then repeats on the other side of the ridge, figures 3(e) and (f). This mechanism of growth will continue if more colloids are deposited.

Starting from the truncated triangles of the first layer, the hexagonal strain field first produces pyramids with clipped edges, as depicted in figures 4(a)–(c). Depositing more colloids, the sites of the missing edges are the nucleation centers of further growth, with small pyramids appearing at the corners of the main pyramid and then filling up the facets between them, figures 4(d)–(e), until finally a pyramid with fully developed sharp corners has formed, figure 4(f). After adding a unidirectional strain component to the hexagonal strain field this interesting growth mechanism via second-order pyramids disappears, figures 5(a)–(f). Now the growth mechanism resembles that of the linear case in figure 3: first an fcc stacking on top of the first layer, followed by an additional filling of more and more facets of the three faces of the pyramidal structure. All three growth mechanisms are found to be independent of the strength λ of the strain.

Strain patterns in different layers. Figure 6 shows the strain fields at different layers of the island depicted in figure 4(d). Moving away from the center of a layer, the strain increases, being zero at the center of the layer and reaching its highest value right at the corners. This pattern is the same for each layer and correlates with the strain field of the substrate,

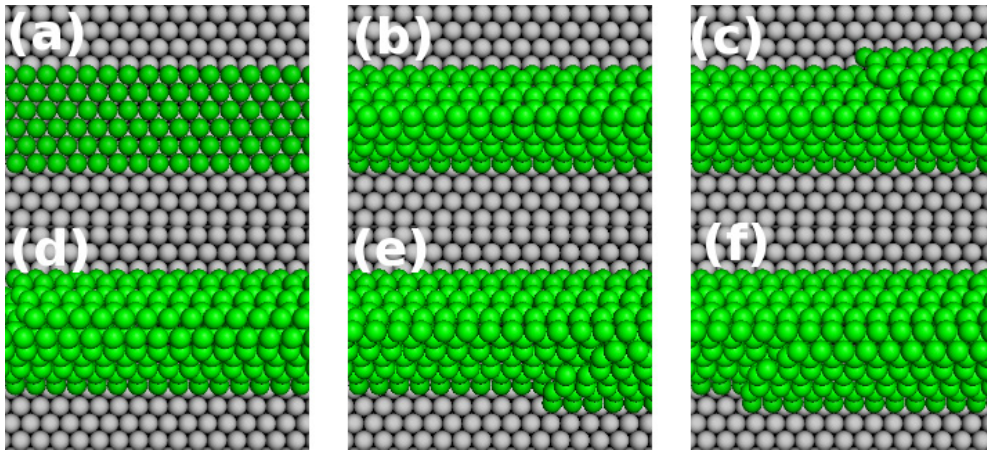


Figure 3. Infinitely extended ridges grow over the linearly strained substrate of figure 2(a1). $\lambda = 0.016$.

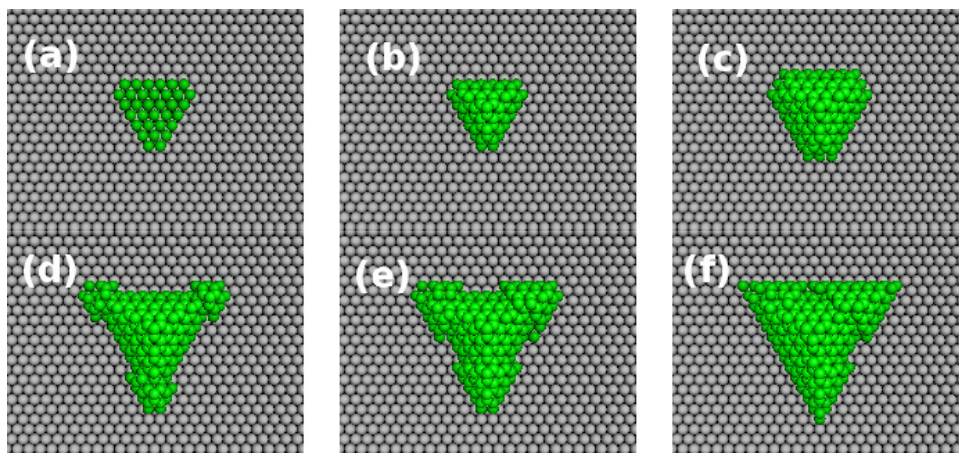


Figure 4. Growth of pyramidal islands with an equilateral triangular base area is induced by a substrate with a hexagonal strain field (strain field in figure 2(b1)). $\lambda = 0.019$.

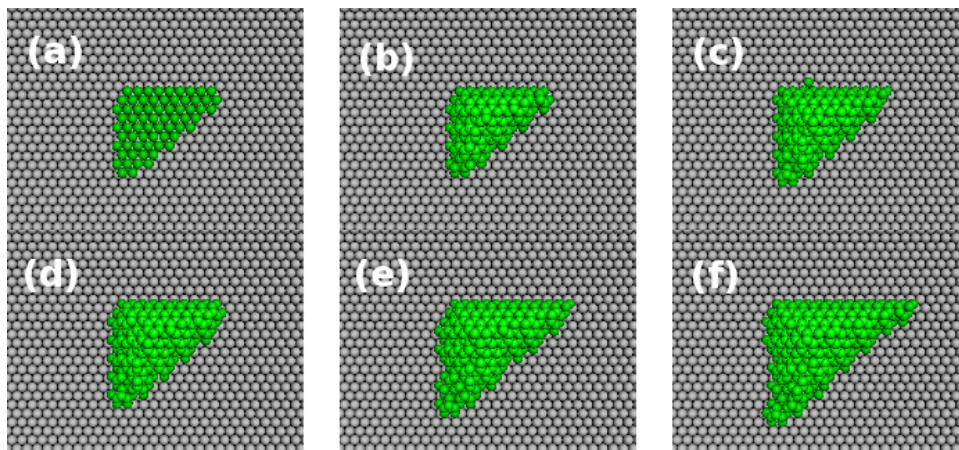


Figure 5. Adding an additional unidirectional strain component to the hexagonal strain field of figure 4, leads to a distortion of the pyramids in figure 4 towards pyramids with a triangular base area having different side lengths (strain field as shown in figure 2(c1)). $\lambda = 0.014$.

figure 2(b1). More importantly, the overall strength of the strain decreases with increasing layer number, demonstrating that the substrate-induced strain is gradually relieved with every new layer. Similar results are obtained for the other

island types. This figure demonstrates that the colloidal growth into the third spatial dimension in the form of islands is simply a way for the system to relax its strain; of course, at the expense of creating more surfaces. The subtle balance between surface

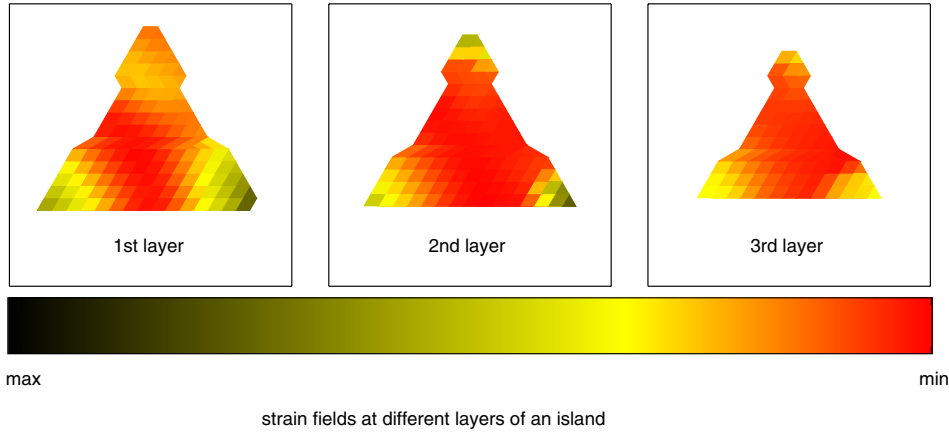


Figure 6. Strain patterns in different layers of the island in figure 4(d), showing zero strain at the center and maximum strain at the corners of each layer.

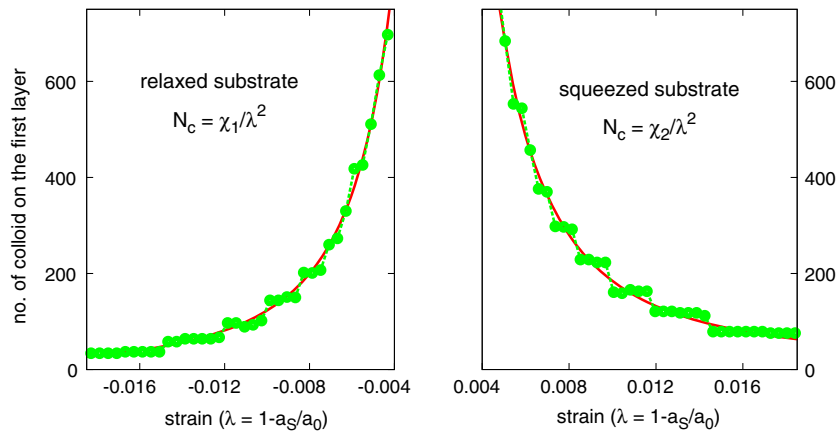


Figure 7. Strain dependence of the first layer area in figure 2(b2) for a substrate with hexagonal strain field as depicted in figure 2(b1).

energy, on the one hand, and the elastic energy stored in the strain pattern, on the other hand, determines the morphological evolution and the final shapes of the islands.

Island size and substrate strain. To give a more quantitative description of the relationship between strain and island size, the number of colloids forming the first layer of the island is correlated in figure 7 with the amount of strain λ , both for relaxed ($\lambda < 0$) and compressed ($\lambda > 0$) substrates. The figure demonstrates that larger strain produces smaller island structures. The two branches for $\lambda < 0$ and $\lambda > 0$ are rather symmetric, both diverging for $\lambda \rightarrow 0$, i.e. both approaching the expected layer-by-layer growth behavior. The curves furthermore suggest that islands grow such that the fraction between the area covered by the island’s first layer and the area $\frac{\sqrt{3}}{2}L^2$ of the repeat unit cell of the periodic strain field is kept constant. In other words, the number N_c of colloids of the first layer should be proportional to $L^2 = 1/\lambda^2$, that is, $N_c = \chi/\lambda^2$. Indeed, a fit to this function (solid curve in figure 7) shows good agreement, resulting in fitting parameters $\chi_1 = 0.0053$ for the relaxed substrate and $\chi_2 = 0.0065$ for the squeezed substrate.

However, the change in island size occurs in discrete jumps, resulting in the observed staircase structure, with

broader stairs at larger strain. Obviously, a given island structure can tolerate small variations in strain, so that with decreasing λ the first layer area grows abruptly only after having reached a certain threshold value. The existence of such threshold values is due to the discrete crystal structure (fcc) that the deposited colloids try to maintain while forming the 3D island structure.

The finding that the island size is inversely proportional to the strain squared has already been predicted in a number of continuum theory calculations [49–52]. But this prediction has not been confirmed by experiments on SiGe/Si(001), showing rather a λ^{-1} dependence [58, 59]. Also, in a very recent study it has been argued that such a λ^{-1} dependence should be more general [53].

6. Final remarks

In this work we have computed minimum-energy island structures of colloidal particles adsorbed on strained surfaces. This paper suggests a colloid experiment in which an attractive colloid pair interaction is induced by the depletion effect while a substrate is prepared by means of optical lattices. We have considered three different strain fields and considered (i) the

relationship between island shape and strain field, (ii) different island growth mechanisms and (iii) the dependence of island size on the strength of strain.

The advantage of our substrate is its flexibility, as it allows to generate rather complex strain patterns which in turn can be used to control the growth and shape of the colloidal islands. We have demonstrated this feature by adding unidirectional strain to a hexagonal strain pattern, resulting in a change of regular pyramidal structures to pyramids with distorted base areas. Such complete control over the strain field is not conceivable for atomic monolayers on real substrates, but represents a rather unique feature of colloidal systems. It could be exploited for more detailed studies on yet inaccessible aspects of the physics of island growth. As an example, we here examined the relation between strain and island size for hexagonal strain fields, finding a λ^{-2} behavior that is a consequence of the fact that the area occupied by an island is a constant fraction of the strain field's repeat unit area. More importantly, the colloid experiment suggested here could be interesting as a self-assembly technique for manufacturing 3D colloidal aggregates in large copy numbers.

Acknowledgment

DD received financial support from the Austrian Science Foundation (FWF) under project title P18762.

References

- [1] Zahn K, Lenke R and Maret G 1999 *Phys. Rev. Lett.* **82** 2721
- [2] Zahn K and Maret G 2000 *Phys. Rev. Lett.* **85** 3656
- [3] von Grünberg H H, Keim P, Zahn K and Maret G 2004 *Phys. Rev. Lett.* **93** 031402
- [4] Zanghellini J, Keim P and von Grünberg H H 2005 *J. Phys.: Condens. Matter* **17** S3579
- [5] Keim P, Maret G and von Grünberg H H 2007 *Phys. Rev. E* **75** 031402
- [6] Baumgartl J, Dietrich J, Dobnikar J, Bechinger C and von Grünberg H H 2008 *Soft Matter* **4** 2199
- [7] Keim P, Maret G, Herz U and von Grünberg H H 2004 *Phys. Rev. Lett.* **92** 215504
- [8] Froltsov V A, Likos C N, Löwen H, Eisenmann C, Gasser U, Keim P and Maret G 2005 *Phys. Rev. E* **71** 031404
- [9] Eisenmann C, Keim P, Gasser U and Maret G 2004 *J. Phys.: Condens. Matter* **16** S4095
- [10] Libal A, Reichhardt C and Olson Reichhardt C J 2007 *Phys. Rev. E* **75** 011403
- [11] Eisenmann C, Gasser U, Keim P, Maret G and von Grünberg H H 2005 *Phys. Rev. Lett.* **95** 185502
- [12] Dobnikar J and Zihel P 2007 *J. Mol. Liq.* **131** 173
- [13] Ebert P, Keim P and Maret G 2008 *Eur. Phys. J. E* **26** 161
- [14] Dillmann P, Maret G and Keim P 2008 *J. Phys.: Condens. Matter* **20** 404216
- [15] Bechinger C and Frey E 2007 *Soft Matter* vol 3, ed G Gompper and M Schick (Weinheim: Wiley-VCH) chapter 2 pp 41–85
- [16] Burns M M, Fournier J M and Golovchenko J A 1990 *Science* **249** 749
- [17] Chowdhury A, Ackerson B J and Clark N A 1985 *Phys. Rev. Lett.* **55** 833
- [18] Brunner M, Bechinger C, Strepp W, Lobaskin V and von Grünberg H H 2002 *Europhys. Lett.* **58** 926
- [19] von Grünberg H H, Helden L, Leiderer P and Bechinger C 2001 *J. Chem. Phys.* **114** 10094
- [20] Meier-Koll A A, Fleck C C and von Grünberg H H 2004 *J. Phys.: Condens. Matter* **16** 6041
- [21] Wei Q H, Bechinger C, Rudhardt D and Leiderer P 1998 *Phys. Rev. Lett.* **81** 2606
- [22] Bechinger C, Wei Q H and Leiderer P 2000 *J. Phys.: Condens. Matter* **12** A425
- [23] Frey E, Nelson D R and Radzihovsky L 1999 *Phys. Rev. Lett.* **83** 2977
- [24] Bechinger C, Brunner M and Leiderer P 2001 *Phys. Rev. Lett.* **86** 930
- [25] Baumgartl J, Brunner M and Bechinger C 2004 *Phys. Rev. Lett.* **93** 168301
- [26] Brunner M and Bechinger C 2002 *Phys. Rev. Lett.* **88** 248302
- [27] Reichhardt C and Olson C J 2002 *Phys. Rev. Lett.* **88** 248301
- [28] Mikulis M, Reichhardt C J O, Reichhardt C, Scalettar R T and Zimanyi G T 2004 *J. Phys.: Condens. Matter* **16** 7909
- [29] Sarlah A, Franosch T and Frey E 2005 *Phys. Rev. Lett.* **95** 088302
- [30] Sarlah A, Frey E and Franosch T 2007 *Phys. Rev. E* **75** 021402
- [31] El Shawish S, Dobnikar J and Trizac E 2008 *Soft Matter* **4** 1491
- [32] Mangold K, Leiderer P and Bechinger C 2003 *Phys. Rev. Lett.* **90** 158302
- [33] Bleil S, von Grünberg H H, Dobnikar J, Castaneda-Priego R and Bechinger C 2006 *Europhys. Lett.* **73** 450
- [34] von Grünberg H H and Baumgartl J 2007 *Phys. Rev. E* **75** 051406
- [35] Baumgartl J, Zvyagolskaya M and Bechinger C 2007 *Phys. Rev. Lett.* **99** 205503
- [36] Chen J X, Cao Y G and Jiao Z K 2004 *Phys. Rev. E* **69** 041403
- [37] Herrera-Velarde S and von Grünberg H H 2009 *Soft Matter* **5** 391
- [38] Herrera-Velarde S and Castaneda-Priego R 2008 *Phys. Rev. E* **77** 041407
- [39] Deb D and von Grünberg H H 2008 *J. Phys.: Condens. Matter* **20** 245104
- [40] Mikhael J, Roth J, Helden L and Bechinger C 2008 *Nature* **454** 501
- [41] Schmiedeberg M, Roth J and Stark H 2006 *Phys. Rev. Lett.* **97** 158304
- [42] Schmiedeberg M and Stark H 2008 *Phys. Rev. Lett.* **101** 218302
- [43] Arciprete F, Placidi E, Sessi V, Fanfoni M, Patella F and Balzarotti A 2006 *Appl. Phys. Lett.* **89** 041904
- [44] Zhu R, Pan E and Chung P W 2007 *Phys. Rev. B* **75** 205339
- [45] Pan E, Sun M, Chung P W and Zhu R 2007 *Appl. Phys. Lett.* **91** 193110
- [46] Ross F M, Tersoff J and Tromp R M 1998 *Phys. Rev. Lett.* **80** 984
- [47] Ross F M, Tromp R M and Reuter M C 1999 *Science* **286** 1931
- [48] Barth J V, Costantini G and Kern K 2005 *Nature* **437** 671
- [49] Srolovitz D J 1989 *Acta Metall.* **37** 621
- [50] Spencer B J, Voorhees P W and Davis S H 1991 *Phys. Rev. Lett.* **67** 3696
- [51] Spencer B J and Blaniariu M 2005 *Phys. Rev. Lett.* **95** 206101
- [52] Levine M S, Golovin A A, Davis S H and Voorhees P W 2007 *Phys. Rev. B* **75** 205312
- [53] Huang Z-F and Elder K R 2008 *Phys. Rev. Lett.* **101** 158701
- [54] Asakura S and Oosawa F 1954 *J. Chem. Phys.* **22** 1255
- [55] Ilett S M, Orrock A, Poon W C K and Pusey P N 1995 *Phys. Rev. E* **51** 1344
- [56] Tuinier R, Rieger J and de Kruif CG 2003 *Adv. Colloid Interface. Sci.* **103** 1
- [57] Fortini A, Dijkstra M and Tuinier R 2005 *J. Phys.: Condens. Matter* **17** 7783
- [58] Sutter P and Lagally M G 2000 *Phys. Rev. Lett.* **84** 4637
- [59] Tromp R M, Ross F M and Reuter M C 2000 *Phys. Rev. Lett.* **84** 4641